Journal of Molecular Structure 1129 (2017) 142–151

Contents lists available at ScienceDirect

Journal of Molecular Structure

journal homepage: http://www.elsevier.com/locate/molstruc

A rapid synthesis of 2-substituted 1,2,3- triazole-1-oxide derivative starting from 4-(methyl)isonitrosoacetophenone and its Ni(II) complex: Characterization, DNA binding and cleavage properties

Ramazan Gup [a, *], Oktay Erer [a], Nefise Dilek [b]

[a] Department of Chemistry, Science Faculty, Mugla Sıtkı Koçman University, 48100 Mugla, Turkey
[b] Department of Physics, Arts and Sciences Faculty, Aksaray University, 68100 Aksaray, Turkey

ARTICLE INFO

Article history:
Received 2 July 2016
Received in revised form
21 September 2016
Accepted 22 September 2016
Available online 23 September 2016

Keywords:
1,2,3-triazole-N-oxide
Oxime
Hydrazine
Nickel(II) complex
DNA binding
DNA cleavage

ABSTRACT

An efficient route, not including any metal salt as a catalyst, for the synthesis of a new 2-substituted 1,2,3- triazole-1-oxide is reported in this paper. The title compound has been synthesized via reacting 4-(methyl)isonitrosoacetophenone with hydrazine hydrate and dipyridyl ketone in high yield under mild reaction condition. The structure of the new 1,2,3-triazole-1-oxide has been characterized via single crystal X-ray and spectral studies. The 1:1 ratio reaction of the 1,2,3-triazole 1-oxide ligand with nickel(II) chloride gives the mononuclear complex $[Ni(L)(DMF)(Cl)_2]$ which is hexa-coordinated within an octahedral geometry. Characterization of the 1,2,3-triazole compound and its Ni(II) complex with FTIR, ^1H and ^{13}C NMR, UV–vis, TGA and elemental analysis also confirm the proposed structures for the compounds. The interactions of the compounds with Calf thymus DNA (CT-DNA) have been investigated via UV–visible spectra and viscosity measurements. The results suggested that both ligand and Ni(II) complex bind to DNA in electrostatic interaction and/or groove binding with a slight partial intercalation. DNA cleavage experiments have been also investigated by agarose gel electrophoresis in the presence and absence of an oxidative agent (H_2O_2). Both 1,2,3-triazole 1-oxide ligand and nickel(II) complex show nuclease activity, which significantly depends on concentrations of the compounds, both in the presence and absence of an oxidative agent. DNA binding and cleavage affinities of the Ni(II) complex is stronger than that of the 1,2,3-triazole 1-oxide ligand.

1. Introduction

Heterocycles containing five-membered rings such as triazole, imidazole, pyrrole, pyrazole, etc., often play an important role in various biochemical processes. Among them triazole derivatives can be ideal drug candidate since they are non-toxic, mostly water soluble and highly stable compounds [1–3]. They have been intensively investigated for many years due to their interesting biological properties, such as antifungal and antibacterial [4–6], anti-nociceptive [7], anti-inflammatory [8], antiviral [9], antituberculosis [10,11], anticancer [12–14] and HIV protease inhibitors [15,16]. Therefore, the synthesis of 1, 2, 3-triazole based heterocycles is the corner stone of drug chemistry because of their broad biological activities. They can also act as N-donor ligands capable of interaction with various metal ions, creating coordination compounds with attractive physico-chemical properties [17,18]. The nitrogen atoms of the 1,2,3-traizole ligands can participate in metal coordination while additional coordination sites can be readily introduced into 2-, 4- or 5- substituents [19–22].

Because of their importance, a number of methods have been developed for the synthesis of 1,2,3-triazole and 1,2,3-triazolium 1-oxide derivatives. The widely used method for the synthesis of 1,2,3-triazole is the copper(I)-catalyzed azide-alkyne cycloaddition, called 'click chemistry', to give 1,4-disubstituted 1,2,3-triazoles in very high yields under mild conditions. This metal-catalyzed reaction discovered independently by Meldal [23] et al. and Sharpless et al. [24] and improved by Huisgen [25,26]. The other common approach to obtain the 1,2,3-triazoles, especially N2-substituted-1,2,3-triazole, is the oxidative cyclization of various hydrazones [27,28]. In the case of the aroylhydrazone-oxime, the oxidative cyclization reaction usually leds to the 1,2,3-triazolium 1-oxides [29–32]. Here we present a new simple one-pot method for the synthesis of the 2-substitue 1,2,3-triazole 1-oxide compounds. We also report an account on synthesis, characterization of nickel(II)

* Corresponding author.
E-mail address: rgup@mu.edu.tr (R. Gup).

http://dx.doi.org/10.1016/j.molstruc.2016.09.066
0022-2860/

complex having N,N,N-1,2,3-triazole 1-oxide ligand moiety and investigation of the DNA binding and cleavage activities of both ligand and its nickel complex.

2. Experimental section

2.1. Material and methods

All the reagents and solvents were of reagent-grade quality and purchased from commercial suppliers. All aqueous solutions were prepared with deionized water, which had been passed through a Millipore Milli-Q Plus water purification system. Calf thymus DNA (CT-DNA) was purchased from Sigma- Aldrich. pBR322 DNA was purchased from Fermantas. ^{1}H and ^{13}C NMR spectra were recorded on a Bruker 400 MHz spectrometer in DMSO_d_6 with TMS as the internal standard. IR spectra were recorded on pure solid samples with a Thermo-Scientific, as KBR pellets. The electronic spectra of the ligands and complexes were recorded on a PG Instruments T80 + UV/Vis Spectrophotometer. Carbon, hydrogen and nitrogen analyses were carried out on a LECO 932 CHNS analyzer and nickel content was determined via atomic absorption spectroscopy using the DV 2000 Perkin Elber ICP-AES. Mass spectra were recorded on a Waters Xevo TQ-S UPLC-MS/MS spectrometer. Room temperature magnetic susceptibility measurements were carried out on powdered samples using a Sherwood Scientific MK1 Model Gouy Magnetic Susceptibility Balance. The thermogravimetric analysis was carried out in dynamic nitrogen atmosphere (20 mL min^{-1}) with a heating rate of 20 °C min^{-1} using a Perkin Elmer Pyris 1 TGA thermal analyzer at Mugla Sitki Kocman University. Crystallographic data were recorded on a Bruker Smart Breeze CCD area-detector diffractometer in Science and Technology Application and Research Center at Aksaray University, Turkey. 4-methylisonitrosoacetophenone [33,34] and 4-methylisonitrosoacetophenone hydrazone [35] were synthesized as described in previously reported methods.

2.2. Synthesis of 2-(di(pyridin-2-yl)methyl)-4-(p-tolyl)-2H-1,2,3-triazole 1-oxide (L)

Dipyridyl ketone (10 mmol, 0.184 g) dissolved in absolute ethanol (30 mL) was added drop wise to a solution of 4-methylisonitrosoacetophenone hydrazone (10 mmol, 0.177 g) in absolute ethanol (20 mL) with a catalytic amount of glacial acetic acid at room temperature. The reaction mixture was refluxed for further 4 h. Then, the reaction mixture was filtered, and the filtrated was allowed at room temperature for crystallization of the 1,2,3-triazole 1-oxide compound. After 4 days, the cream crystals suitable for X-ray diffraction were formed, collected by filtration, washed with small amount of diethyl ether and then dried in vacuum. The ligand is soluble in common organic solvents and insoluble in water.

Yield 85%; Mp 175–176 °C; UV (DMF, nm) 268 and 324; IR (KBr, cm^{-1}) 3149 (triazole), 3043, 2947 (C–H), 1588 and 1525 (C=N), 1188 (C–N), 945 (N–O); ^{1}H NMR (DMSO_d_6, ppm) δ 2.34 (s, 3H), 7.31 (d, 2H Ar–H), 7.35 (m, 2H, Py-H), 7.45 (m, 2H, Py-H), 7.49 (s, H C–H), 7.65 (d, 2H, Ar–H), 7.85, (m, 2H, Py-H), 8.40 (s, H, CH=N), 8.60 (m, 2H, Py-H); ^{13}C NMR (DMSO_d_6, ppm) 155, 149, 144 (C=N), 139, 137, 129.5, 126, 125, 123.5, 123.6, 113 (Ar–C), 66 (C–N), 21 (CH_3). Analysis (% calculated/found) for $C_{20}H_{17}N_5O$ C: 69.96/70.24, H: 4.99/4.98, N: 20.40/20.43.

2.3. Synthesis of Ni(II) complex ([Ni(L)(DMF)Cl_2])

A solution of 1 mmol $NiCl_2 \cdot 6H_2O$ (0.2377 g) in EtOH (10 mL) was added to a hot solution containing 1 mmol ligands (0.343 g) in absolute ethanol (15 mL) with stirring. The reaction mixture was refluxed for 2 h, and then the resulting green precipitate was filtered off, washed with absolute ethanol and small amount of cold water, and then dried in vacuum. The crystals, unsuitable for X-ray diffraction, were obtained upon diffusion of the ethyl ether into the DMF solution after 3 weeks. Yield: 76%; M.p.: 277 °C. UV (DMF, nm); 270 and 348; FT-IR (KBr, cm^{-1}) 3429, 3112 (triazole), 3031, 2942, (C–H), 1643 (C=O), 1605 and 1498 (C=N), 1189 (C–N), 947 (N–O); Analysis (%calculated/found) for $C_{23}H_{24}Cl_2N_6NiO_2$ C: 50.59/50.92, H: 4.43/4.48, N:15.39/15.44, Cl: 12.98/12.69, Ni: 10.75/10.24.

2.4. X-ray diffraction study

Crystallographic data were recorded on a Bruker Smart Breeze CCD diffractometer using MoK_α radiation (λ = 0.71073 Å) at T = 296(2) K [36]. Absorption corrections by multi-scan were applied [36,37]. Cell refinement was carried out using Bruker SAINT and data were reduced by using Bruker SAINT [36]. The structure was solved using SHELXS97 [38] and refined using SHELXL2014 [39] by full-matrix least-squares on F^2 against ALL reflections. The weighted R-factor wR and goodness of fit S are based on F^2. The threshold expression of $F^2 > 2sigma(F^2)$ is used only for calculating R-factors. All estimated standard deviations (e.s.d.'s) are calculated using the full covariance matrix. The cell e.s.d.'s is taken into account individually in the estimation of e.s.d.'s in distances, angles, and torsion angles; correlations between e.s.d.'s in cell parameters are only used when they are defined by crystal symmetry. Molecular graphics were drawn ORTEP-3 [40] and PLATON [40], and the material for publication prepared using WinGX [41]. All non-hydrogen atoms were refined anisotropically and hydrogen atoms were added according to the theoretical model. A summary of the experimental details and selected results for the title compound are given in Table 1. The fractional atomic coordinates are given in Table S1 and also the selected bond distance, bond angles, and torsion angles are given in Table 2.

2.5. DNA binding

2.5.1. Electronic absorption titrations

All the experiments involving the interaction of the complexes with CT-DNA were carried out in water buffer containing 5 mM tris [tris(hydroxymethyl)aminomethane] and 50 mM NaCl, and adjusted to pH 7.3 with HCl. The solution of CT-DNA in the buffer gave a ratio of UV absorbance of 1.8–1.9:1 at 260 and 280 nm, indicating that the CT-DNA was sufficiently free of protein [42]. The CT-DNA concentration per nucleotide was determined spectrophotometrically by employing an extinction coefficient of 6600 M^{-1} cm^{-1} at 260 nm [43]. An appropriate amount of the compound was dissolved in a solvent mixture of 1% DMF and 99% tris–HCl buffer. Absorption titration experiments were performed by maintaining the compound concentration as constant (25 μM) while the concentration of the CT-DNA gradually increased within 6.25–50 μM.

2.5.2. Viscosity measurements

Viscosity experiments were carried out using an Ubbelodhe viscometer at room temperature. The viscosity of CT-DNA solution (25 μM) was measured in the absence and presence of increasing amounts of the compound (6,25–50 μM) in tris-HCl buffer (10 mM tris–HCl-NaCl; pH = 7.6) containing %5 DMF solution. Flow time was measured three times via a digital stopwatch. Viscosity values were presented as $(\eta/\eta_0)^{1/3}$ versus concentrations of [complex]/[DNA] [44,45] where η was the viscosity value for DNA in presence of the compounds and η_0 was the viscosity value of CT-DNA alone.

Table 1
Crystal data and structural refinement details.

Chemical formula	$C_{20}H_{17}N_5O$
Formula weight (amu)	345.40
Crystal form, color	yellow, colourless
Crystal size (mm)	0.980 × 0.740 × 0.450
Crystal system	Triclinic
Space group	*P-1*
a (Å)	8.9288(2)
b (Å)	9.9399(3)
c (Å)	10.6983(3)
α (°)	70.003(1)
β (°)	89.542(1)
γ (°)	72.276(1)
V (Å^3)	844.98(4)
Z	2
D_x (g/cm^3)	1.358
λ(MoK_α) Å	0.71073
μ(MoK_α) mm^{-1}	0.088
T (K)	296(2)
θ $_{max}$	28.43
θ $_{min}$	2.30
h	−11–11
k	−13–13
l	−14–14
Number of reflections measured	20762
Number of independent reflections	4275
Number of reflections [$I > 2\sigma(I)$]	3781
Number of parameters	237
R	0.0490
Rw	0.1207
S	1.012
Weighting scheme,	$1/[\sigma^2(F_o^2) + (0.1040P)^2$ $P = (F_o^2 + 2F_c^2)/3$
$(\Delta/\sigma)_{max}$	0.041
$(\Delta\rho)_{max}$, $(\Delta\rho)_{min}$ (eÅ^{-3})	0.286, −0.245
Measurements	Bruker Smart Breeze
Structure determination	direct method (SHELXS-97)
Refinement	full matrix l.s. (SHELXL-2014)
Treatment of hydrogen atoms	geometric calculation

2.6. Chemical nuclease activity

pBR322 plasmid DNA was used for all cleavage activities. In a typical experiment, 7 μl plasmid DNA (50 ng/μl) was mixed with different concentrations of complexes (10, 25, 50, 75 and 100 μM dissolved in DMF) to determine optimum activation concentration. 5 μl H_2O_2 (5 mM) was added to mixture to oxidize the reactant. Finally, the reaction mixture was diluted with the Tris buffer (100 mM Tris, pH: 8) to a total volume of 30 μl. After that reaction mixtures were incubated at 37 °C for 2 h. Samples (20 μl) were then loaded with 4 μl loading dye (0.25% bromophenol blue, 0.25% xylene cyanol, 30% glycerol, 10 mmol EDTA) on a %1 agarose gel containing 1 μg/mL of EtBr. The gel was run at 100 V for 3 h in TBE buffer and photographed under UV light.

3. Results and discussion

3.1. Synthesis and characterization

In this study a new 1,2,3-triazole-N-oxide ligand was synthesized in a one-step reaction of 4-(methyl)isonitrosoacetophenone hydrazone with di(2-pyridyl)ketone in presence of a catalytic amount of acetic acid as illustrated in Scheme 1. We suggest that the partly environment-friendly reaction proceeds via an intermediate asymmetric azine compound which quickly undergoes cyclization in the presence of catalytic amount of acetic acid to produce 1,2,3-triazole 1-oxide compound in high yield under mild conditions. The crystal structure of the 1,2,3-triazole 1-oxide was defined by using single crystal X-ray diffraction analysis corresponding to the proposed formula of the compound, which is also supported by FTIR, UV–Vis, ^{1}H NMR, ^{13}C NMR and elemental analysis. The Ni(II) complex was synthesized by the reaction of the 1,2,3-triazole-N-oxide ligand with nickel(II) chloride in ligand to nickel ratio of 1:1. The nature of bonding and geometry of the Ni(II) complex was deduced from elemental analysis, FTIR and UV–Vis spectroscopies, magnetic susceptibility measurement and thermal gravimetric analysis techniques.

The electronic spectra of the ligand and Ni(II) complex were taken in dimethylformamide. The free ligand shows bands at 268 and 324 nm. These bands are due to aromatic nature of the 1,2,3-triazole-N-oxide ligand. The Ni(II) complex on the other hand shows a band at 270 nm and a shoulder at 348 nm probably due to π-π* and n-π* transitions [46,47]. Unfortunately, the expected weak d–d transition in the visible region for the complex cannot be detected even with concentrated solution. It may be lost in the low energy tail of the charge transfer transition. The observed magnetic moment (μ_{eff}) is 2.92 BM for the nickel complex and is consistent with its octahedral geometry (Fig. 1) [48].

^{1}H NMR of the 1,2,3-triazole-N-oxide ligand exhibits bands between 7.30 and 8.60 ppm due to the pyridine ring protons. The observed doublet-doublet peaks, resembling an AB pattern of two distorted doublets, at 7.31 and 7.65 ppm belong to 1,4-disubstitue benzene protons side of the compound. The characteristic signal of triazole ring appears at 8.60 ppm whereas the methine proton, adjacent to N3 atom (Fig. 3), appears as a singlet at 7.49 ppm. The movement of this absorption to lower frequency can be explained by an inter-molecular hydrogen bond between this hydrogen atom with acceptor N1 atom. The absence of the OH proton signal indicates the deprotonation of the hydroxyl proton and subsequent formation of 1,2,3-triazolium salt. The ^{1}H NMR spectral assignments of the 1,2,3-triazol 1-oxide ligand are also supported by the ^{13}C NMR spectrum. The characteristic chemical shifts for the azomethine groups are observed at 155, 149 and 144 ppm. The chemical shifts for the carbon atoms of the aromatic rings are recorded between 113 and 139 ppm. In the ^{13}C NMR spectra of the

Table 2
Selected bond lengths (Å), bond angles (°) and torsion angles (°).

Bond lengths		Bond angles		Torsion angles			
O1–N5	1.275(1)	N4–N3–N5	112.18(9)	N5–N3–N4–C13	−2.1(1)	C2–C1–C6–N3	77.6(1)
N3–N4	1.335(1)	N4–N3–C6	127.43(9)	C6–N3–N4–C13	−170.0(1)	N1–C1–C6–C7	130.1(1)
N3–N5	1.359(1)	N5–N3–C6	119.31(9)	C6–N3–N5–O1	−9.2(2)	C2–C1–C6–C7	−46.3(1)
N3–C6	1.462(1)	N3–N4–C13	104.68(9)	N4–N3–N5–C12	1.7(1)	N3–C6–C7–N2	−32.7(1)
N4–C13	1.340(1)	O1–N5–C12	132.0(1)	C6–N3–N5–C12	170.7(1)	C1–C6–C7–N2	91.5 (1)
N5–C12	1.337(2)	O1–N5–N3	121.5(1)	C6–C1–N1–C5	−174.8(1)	N3–C6–C7–C8	149.0(1)
N1–C1	1.333(1)	C12–N5–N3	106.5(1)	N4–N3–C6–C7	105.8(1)	C1–C6–C7–C8	−86.9(1)
N1–C5	1.342(2)	C1–N1–C5	117.1(1)	N5–N3–C6–C7	−61.4(1)	C19–C14–C13–N4	3.0(2)
N2–C7	1.333(1)	C7–N2–C11	116.6(1)	N4–N3–C6–C1	−19.1(2)	C15–C14–C13–N4	−177.3(1)
N2–C11	1.342(2)	N3–C6–C7	110.51(8)	N5–N3–C6–C1	173.78(9)	C19–C14–C13–C12	−176.5(1)
		N3–C6–C1	110.82(8)	N1–C1–C6–N3	−106.0(1)	C6–C1–C2–C3	175.5(1)

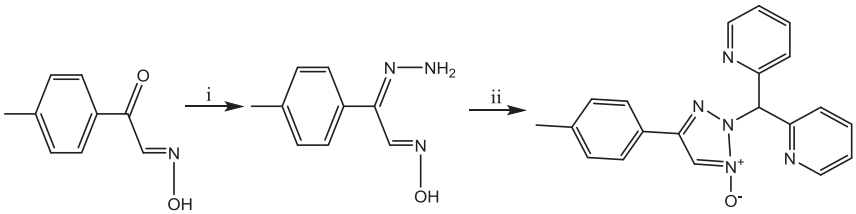

Scheme 1. Schematic diagram showing the synthesis of the 1,2,3-triazole-N-oxide ligands. **i**, NH_2NH_2, room temperature; **ii**, di(2-pyridyl) ketone, EtOH, AcOH, reflux 4 h.

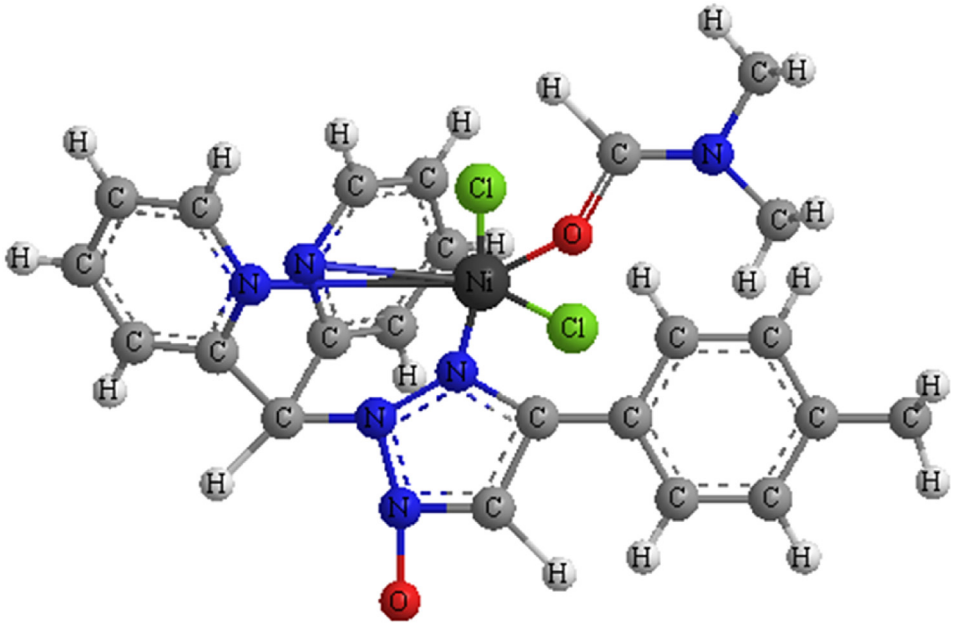

Fig. 1. Proposed structure for the Ni(II) complex.

ligand, the signals at 66 and 21 ppm are assignable to the C—N and CH_3 groups, respectively.

The IR spectra of the 1,2,3-triazole n-oxide compound show sharp stretching vibration peaks at 3149, 3043, 2947, 1588 and 1525, 1188 and 945 cm^{-1} due to ν(C—H) triazole, ν(C—H) aromatic, ν(C—H) aliphatic, ν(C═N), ν(C—N) and ν(N—O) groups, respectively. Upon coordination of Ni(II) ion, the vibration bands of ν(C═N) bounds are observed at 1605 and 1498 cm^{-1} indicating the involvement of these groups in the complex formation. Furthermore, in the IR spectra of the Ni(II) complex a new absorption

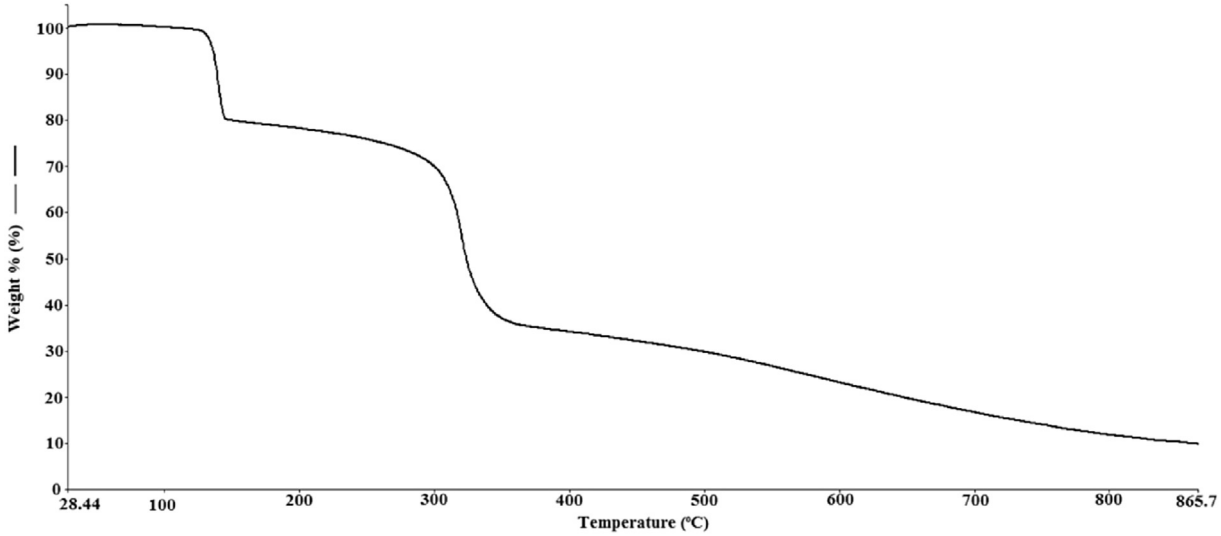

Fig. 2. TGA curve of the nickel(II) complex.

appears at 1643 cm^{-1} due to stretching vibration of the carbonyl group of the coordinated dimethylformamide. The magnetic measurement, elemental analysis and FT-IR data indicate that the 1,2,3-triazole n-oxide compound act as a neutral *N,N,N*-tridentate ligand coordinating through two pyridine nitrogen atoms and one triazole nitrogen atom, and the structure proposed for the nickel(II) complex is given in Fig. 1.

Temperature stability of the nickel(II) complex was conceived by using thermogravimetric (TG) method carried out from 20 to 865 °C (Fig. 2). TG curve exhibits mass losses in three steps. The first step occurs within the temperature range 130–264 °C, which corresponds to the removal of two chloride ions and one dimethylformamide molecule, with a mass loss of 23.40% (calcd: 23.81%). The subsequent steps (264-865 °C) correspond to the removal of the organic part of 1,2,3-triazole 1-oxide ligand, leaving metal oxide as a residue.

3.2. Description of the crystal structures

Crystal structure was obtained for the 2-(di(pyridin-2-yl) methyl)-4-(p-tolyl)-2H-1,2,3-triazole 1-oxide and it is discussed below. The selected geometric parameters are listed in Table 1. The new 1,2,3-triazole compound crystallized in the triclinic *P-1* space group. The crystal structure is shown in Fig. 3 with atom-numbering scheme, and the selected bond lengths and bond angels are summarized in Table 2. The N3–C6 bond length is 1.462(1) Å corresponding to C–N single bond length, whereas the other C–N bond lengths range from 1.333(1) to 1.342(2) Å which are between the C–N single (1.471 Å) and double (1.273 Å) bonds and similar with the reported 1,2,3-triazole compounds (1.309–1.339 Å) [49,50] Similarly, the N3–N4 and N3–N5 distances are 1.335(1) and 1.359(1) Å, respectively, which are half way between being a single (N–N) and a double (N=N) [51,52]. These observed bond lengths indicate that the synthesized 1,2,3-triazole has resonance structures. The O1–N5 bond distance is 1.275(1) Å which is shorter than a half bond character, surprisingly. Since there are opposite charges on side to side N5 and O1 atoms of the 1,2,3-triazole compound, the possible ionic interaction beside covalent interaction may be reason of this observed bond length. The other bond lengths and angles in the molecule are within expected ranges, and similar to the other studies [49–52]. The all chelate rings of molecule are essentially planar. The dihedral angle between A (N1/C1–C5) and B (N2/C7–C11) planes is 80.64 (4)°. These two rings are close to perpendicular. The dihedral angle between A and C (N3–N5/C12, C13) planes is 63.07 (4)°. The dihedral angle between B and C planes is 78.27 (5)°. The dihedral angle between C and D (C14–C19) is 3.64 (10)°. These rings are almost in the same plane. The O1 atom lies below 0.026 (2) Å from C plane. The C6 atom lies below 0.197 (2) Å and 0.053 (2) Å from C and B planes, respectively. Also, the C6 atom lies above 0.120 (2) Å from A plane. The C14 atom lies above 0.036 (2) Å from C plane. The C13 and C20 atoms lie above 0.043 (2) and 0.024 (3) Å from D plane, respectively.

The H atoms were positioned geometrically with C–H = 0.93 Å (aromatic), C–H = 0.96 Å (methyl), C–H = 0.98 Å (for C6) and constrained to ride on their parent atoms, with $U_{iso}(H) = 1.2U_{eq}(C_{aromatic}, C6)$ and $U_{iso}(H) = 1.5U_{eq}(C_{methyl})$.

As can be seen from the packing diagram (Fig. 4), intermolecular C–H … π hydrogen bonds (Table S2) link the molecules and these hydrogen bonds may be effective in the stabilization of the crystal structure. In this interaction, the N1 atom acts as an acceptor and C6 atom acts as a donor.

3.3. Binding studies

3.3.1. Electronic absorption titrations

Electronic absorption spectroscopy is one of the most widely used techniques to monitor the interaction of metal complexes with DNA. Metal complexes can bind to DNA through both covalent and/or non-covalent interactions [49,50]. In covalent interactions a nitrogen donor atom from the nucleotide binds to the metal complexes or it is replaced the labile group of complexes, while non-covalent interactions occur via intercalative, electrostatic and groove binding. Hypochromism results from the contraction of DNA in the helix axis, as well as from the change in conformation on DNA. On the other hand, hyperchromism in absorption bands indicate minor groove binding, unwinding of DNA double helix, simultaneous exposure of the DNA bases and damage to the DNA double helix [53–56].

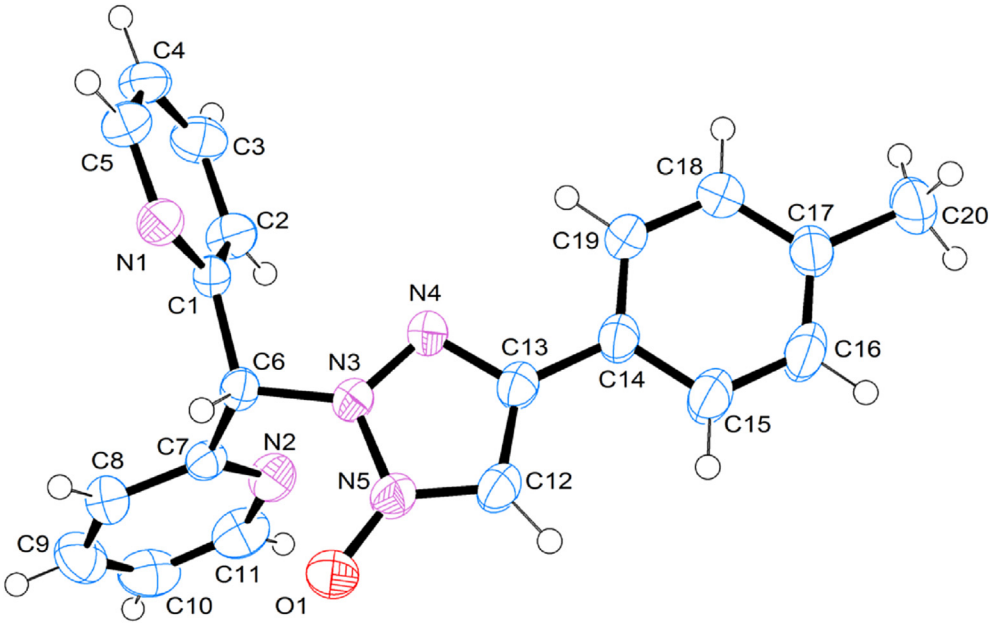

Fig. 3. An ORTEP drawing of molecular structure with the crystallographic numbering scheme. Thermal ellipsoids are drawn at % 50 probability levels.

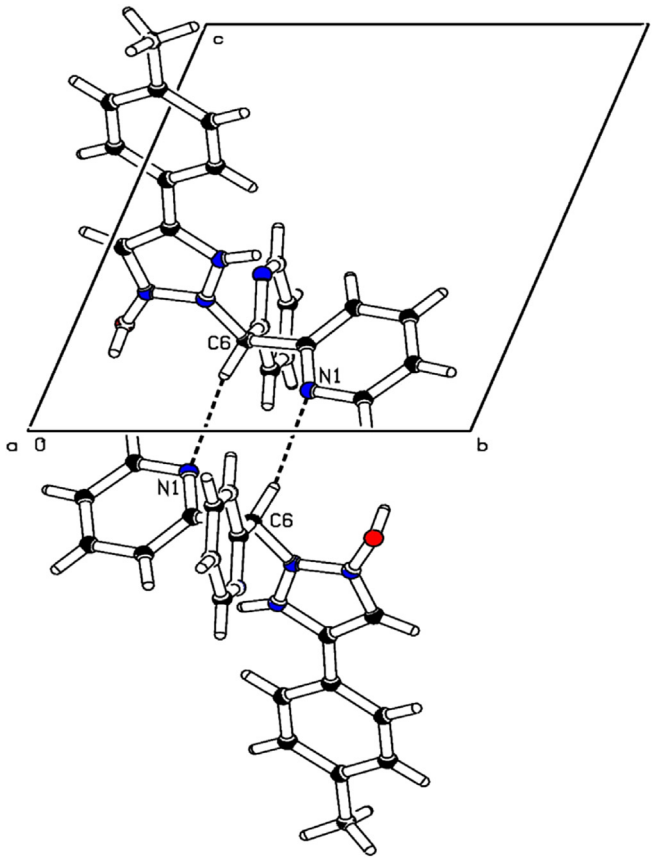

Fig. 4. A packing diagram for molecule, projected along *a* direction. Hydrogen bonds are indicated by dashed lines.

The absorption spectra of the ligand and its Ni(II) complex (25 μM) in the presence of different concentrations of CT-DNA (6.25–50 μM) are shown in Figs. 5 and 6. The absorption peaks observed at 268 and 323 nm for 1,2,3-triazole 1-oxide ligand and 270 and 348 nm for Ni(II) complex can be attributed π-π* and n- π* transitions, respectively. With increasing concentration of CT-DNA, for the ligand, the hyperchromism in the peak at 268 nm reaches as high as 38.8% with as small bothochromism of 2 nm. The nickel (II) complex also exhibits an evident hyperchromism of about 50.5% at 270 nm and red shift of 2 nm. A strong hyperchromic effect in π-π* transition was observed for the Ni(II) complex suggesting that it has higher propensity for DNA binding than the 1,2,3-triazole ligand. The absorption spectra of both 1,2,3-triazole 1-oxide ligand and its Ni(II) complex exhibits hyperchromism upon addition of CT-DNA which is suggestive of a conformational change of the DNA duplex [57]. Hyperchromic effect may also be due to the electrostatic interaction between positively charged N (5) atom of the triazole moiety of the compounds and negatively charged phosphate backbone at the periphery of the double helix DNA [42,43]. On the other hand, during this interaction the repulsion can take place between the negatively charged O (1) atom of the compounds and negatively charged phosphate group of CT-DNA which probably diminishes the force of the electrostatic interaction as well as DNA binding abilities of the compounds. Structurally, electrostatic binding may not be one of the binding mode, since the 1,2,3-triazole 1-oxide ligand has planar area and extended system, thereby leading to penetration and binding within DNA base pairs. Nevertheless, the complete intercalation of the compounds between a set of adjacent base pairs is impossible probably due to the strong attraction and repulsion between positively (N5) and negatively (O1) charged atoms of the compounds with negatively charged phosphate, yet some partial intercalation can be proposed [58–60]. The existing 1,2,3-triazole 1-oxide ligand and its Ni(II) complex may bind to DNA by groove binding since they have many hydrogen bonding cites which may form hydrogen bonds with DNA double helix. On the other hand, the existing compounds bearing methyl group can also bind to DNA via a van der Waals interaction between methyl group of the 1,2,3-triazole 1-oxide ligand and DNA base thymine.

The binding constant, K_b, was determined by using the equation, $[DNA] / (\varepsilon_a - \varepsilon_f) = [DNA] / (\varepsilon_o - \varepsilon_f) + 1 / Kb\,(\varepsilon_o - \varepsilon_f)$, where [DNA] is the concentration of DNA in base pairs, ε_a, ε_f and ε_o correspond to $A_{obsd}/[M]$, the extinction coefficient of the complexes and the

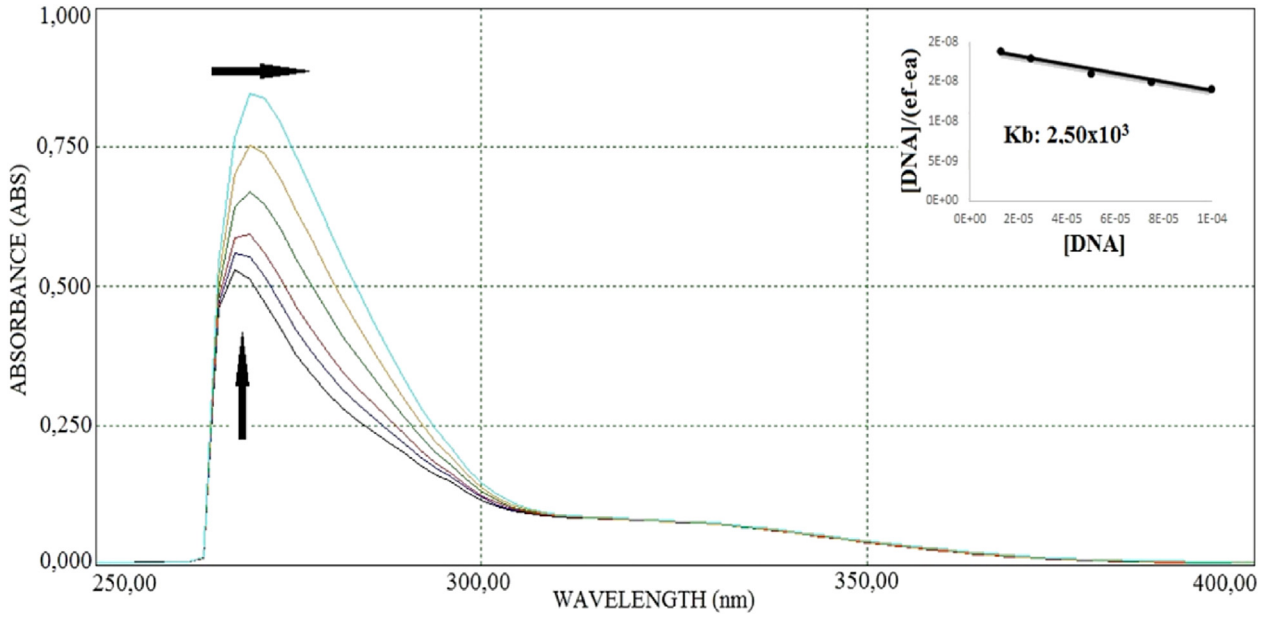

Fig. 5. Absorption spectral traces of the 1,2,3-triazole-N-oxide ligand with increasing concentration of CT-DNA.

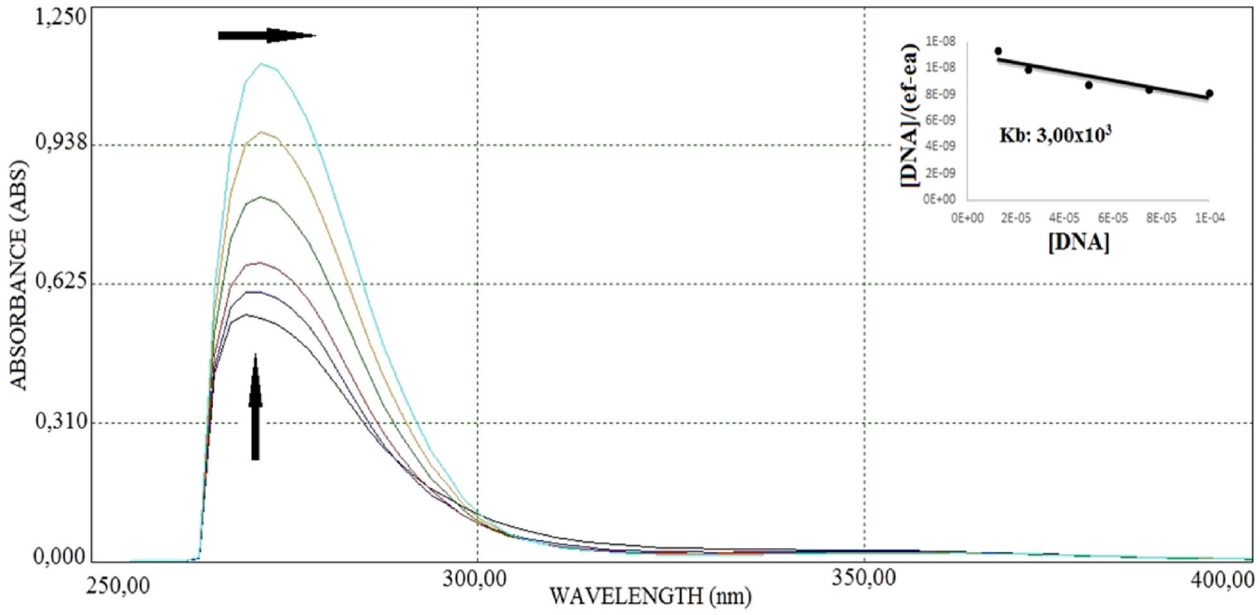

Fig. 6. Absorption spectral traces of the nickel(II) complex with increasing concentration of CT-DNA.

extinction coefficient of the complex in the fully bound form, respectively, and K_b is the intrinsic binding constant. The ratio of the slope to intercept in the plot of [DNA] / $(\varepsilon_a - \varepsilon_f)$ versus [DNA] gives the value of K_b and for complex. The binding constant (K_b) values of $2.5 \times 10\ M^{-1}$ for the ligand and $3.0 \times 10^3\ M^{-1}$ for the Ni(II) complex suggest that the complex has slight higher affinity to DNA than that of the ligand. These lower values also indicated partial intercalative binding and/or surface binding of the complexes to DNA.

3.3.2. *Viscosity measurements*

To understand the nature of the interaction between the compounds and DNA, viscosity measurements were also performed. Viscosity parameter is important as it sensitive to the change in length of DNA strands and provides valuable information for any conformational change. A strong intercalation of the ligand leads to lengthening of DNA helix as base pairs are separated to accommodate the binding ligand, leading to an increase in viscosity of the DNA solution. In contrast, electrostatic interaction, groove binding or partial intercalation leads to only minor changes in the viscosity [61,62]. The binding modes of the 1,2,3-triazole 1-oxide ligand and nickel(II) complexes to DNA are further confirmed via viscosity measurement carrying out by keeping [DNA] = 25 mM and varying the concentrations of the 1,2,3-triazole-1-oxide and its Ni(II) complexes, DAPI or EB. The results are shown in Figs. 7 and 8. The EB and DAPI have been used as references. As it can be seen from these Figures, ethidium bromide (EB), being a well-known DNA intercalator between DNA base pairs and thus lengthening the DNA double helix, increases the relative viscosity of DNA sharply whereas the viscosity of double strand DNA remains almost unchanged in the case of DAPI, minor groove binding agent [60,63].

Here, the relative viscosity of DNA solutions slightly increases upon increasing the amounts of 1,2,3-triazole-N-oxide ligand while it is almost unchanged in the case its nickel(II) complex. The results indicate electrostatic and/or groove binding nature of Ni(II) complex and also partial intercalative nature of 1,2,3-triazole 1-oxide ligand, which is also in agreement with the result of absorption spectra. This situation may be related to the molecular structures of the compounds. The 1,2,3-triazole 1-oxide has planar geometry,

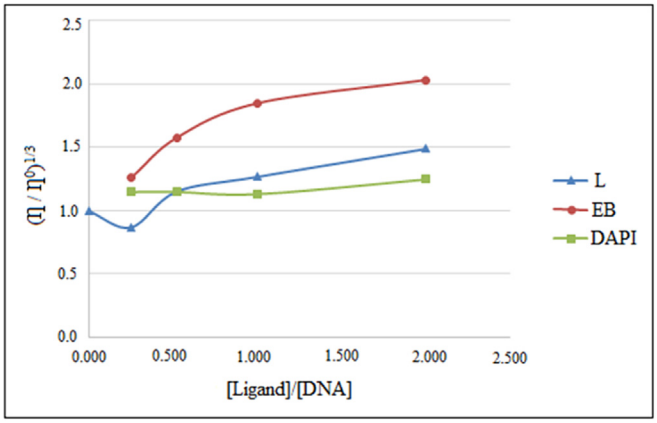

Fig. 7. Effect of increasing amounts of the 1,2,3-triazole 1-oxide ligand, DAPI and EB on the relative viscosity of calf thymus DNA at room temperature.

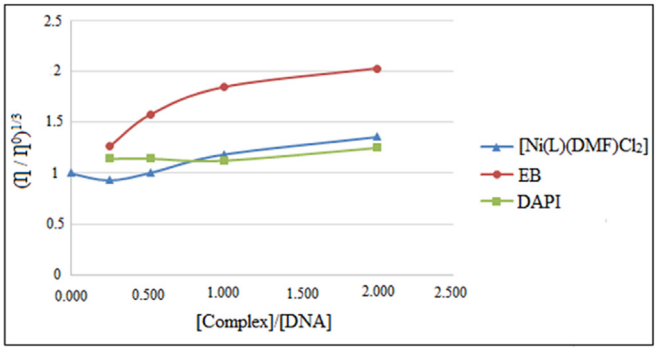

Fig. 8. Effect of increasing amounts of the Ni(II) complex, DAPI and EB on the relative viscosity of calf thymus DNA at room temperature.

and easily penetrate into DNA base pairs binding to DNA probably through a stacking interaction between the aromatic chromophore of the ligand and the base pairs of DNA. On the other hand, the nickel(II) complex has been proposed to have an octahedral

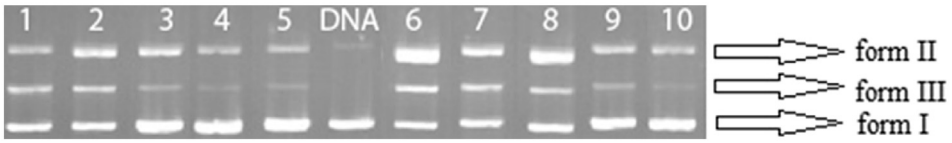

Fig. 9. Agarose gel electrophoresis of pBR322 plasmid DNA by different concentrations of the 1,2,3-triazole-1-oxide ligand (L) in the presence and absence of hydrogen peroxide. Lane 1: [L] (200 μM) + DNA + H_2O_2, Lane 2: [L] (100 μM) + DNA + H_2O_2, Lane 3: [L] (75 μM) + DNA + H_2O_2, Lane 4: [L] (50 μM) + DNA + H_2O_2, Lane 5: [L] (25 μM) + DNA + H_2O_2, Lane 6: [L] (200 μM) (10 μM) + DNA, Lane 7: [L] (100 μM)) + DNA, Lane 8: [L] (75 μM) + DNA, Lane 9: [L] (50 μM) + DNA, Lane 10: [L] (25 μM) + DNA.

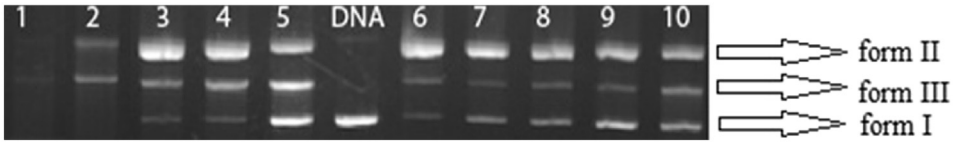

Fig. 10. Agarose gel electrophoresis of pBR322 plasmid DNA by different concentrations of the Ni(II) complex [Ni(L)(DMF)Cl_2] in the presence and absence of hydrogen peroxide. Lane 1: [Ni(L)(DMF)Cl_2] (200 μM) + DNA + H_2O_2, Lane 2: [Ni(L)(DMF)Cl_2] (100 μM) + DNA + H_2O_2, Lane 3: [Ni(L)(DMF)Cl_2] (75 μM) + DNA + H_2O_2, Lane 4: [Ni(L)(DMF)Cl_2] (50 μM) + DNA + H_2O_2, Lane 5: [Ni(L)(DMF)Cl_2] (25 μM) + DNA + H_2O_2, Lane 6: [Ni(L)(DMF)Cl_2] (200 μM) (10 μM) + DNA, Lane 7: [Ni(L)(DMF)Cl_2] (100 μM)) + DNA, Lane 8: [Ni(L)(DMF)Cl_2] (75 μM) + DNA, Lane 9: [Ni(L)(DMF)Cl_2] (50 μM) + DNA, Lane 10: [Ni(L)(DMF)Cl_2] (25 μM) + DNA.

geometry that, in part, relieves the steric crowding of the coordinated ligands. This steric structure of the nickel complex may hinder the intercalation mode in between the base pair of DNA.

3.4. Cleavage studies

The chemical nuclease activities of the compounds have been studied by using pBR322 plasmid in TBE buffer at 37 °C in the presence and absence of oxidizing agent under similar physiological conditions. When pBR322 is conducted by electrophoresis, the fast migration will be observed for the supercoiled form (Form I). If only one DNA strand is cleaved, the form I will relax to produce a slower-moving nicked circular from (Form II). If both strands are cleaved, a linear form (Form III) that migrates at a rate between that of Form I and Form III will be produced. Figs. 9 and 10 exhibit the results of gel electrophoretic separations of pBR322 plasmid induced by an increasing concentration of the compounds (25–200 μM) in the presence and absence of hydrogen peroxide. The results show that both ligand and its Ni(II) complex behave as a chemical nuclease activity by nicking Form I into Form II and Form III in the presence and absence of hydrogen peroxide. The increasing concentrations of the compounds led to a gradual diminish in the band intensity of Form I, while partly increasing in the band intensities of Form II and Form III progressively suggesting double-strand DNA breaks. The results also indicate that the nickel complex exhibits better and different DNA cleavage affinity from 1,2,3-triazole 1-oxide ligand. It converts mostly the supercoiled DNA to nicked and linear DNA even in the low concentrations (50 μM) both in the presence and absence of an oxidative agent. In the presence of hydrogen peroxide, with 100 μM the nickel(II) complex is found to completely cleave Form I to Form II and Form III (Fig. 10, lane 2) and at the 200 μM concentration of the Ni(II) complex, the plasmid DNA is almost degraded into indistinguishable small fragments. In the absence of hydrogen peroxide the nickel(II) complex also shows effective nuclease activity. With the increase of the Ni(II) complex concentration, the intensity of the supercoiled DNA band is found decrease gradually while those of nicked and linear DNA bands increase apparently (Fig. 10, lanes 6-10) and finally the supercoiled DNA almost disappears at 200 μM concentration.

4. Conclusions

In this study, we report a convenient route for the synthesis of a new heterocyclic compound incorporating 1,2,3-triazole 1-oxide moiety in order to investigate its coordination behavior and DNA interaction ability. The one-pot reaction was carried out in a yield of 85% in a single reactor by the interaction of 4-(methyl)isonitrosoacetophenone, hydrazine hydrate, di-2-pyridyl ketone, acetic acid in ethanol without using any metal salt as a catalyst. Its coordination ability was tested with bio relevant Ni(II) ion which occupies a six coordinated octahedral environment surrounded by the two pyridyl nitrogen atoms and one nitrogen atom of the 1,2,3-triazole ring of N,N,N-tridentate ligand, two chloride ions and one dimethylformamide group. The results of electronic absorption titrations and viscosity measurements indicate that both 1,2,3-triazole 1-oxide ligand and its Ni(II) complex interact with CT-DNA through the non-covalent binding mode possibly by the electrostatic interaction and/or groove binding as well as the partial intercalation. The compounds exhibit efficient nuclease activity in the presence and absence of hydrogen peroxide which has dependence on the concentration of compound. The results also indicate that the chemical nuclease activity of the nickel complex is nakedly higher than that of its 1,2,3-triazole 1-oxide ligand probably due to its higher DNA binding affinity.

Acknowledgements

We thank the Scientific Research Projects Foundation of Mugla Sıtkı Koçman University for financial support of this work (BAP No: 13-169).

Appendix A. Supplementary data

Supplementary data related to this article can be found at http://dx.doi.org/10.1016/j.molstruc.2016.09.066.

References

[1] J.M. Kumar, M.M. Idris, G. Srinivas, P.V. Kumar, V. Meghah, M. Kavitha, C.R. Reddy, P.S. Mainkar, B. Pal, S. Chandrasekar, N. Nagesh, Phenyl 1,2,3-Triazole-Thymidine ligands stabilize g-quadruplex DNA, inhibit DNA synthesis and potentially reduce tumor cell proliferation over 3′-Azido deoxythymidine, Plos One 8 (2013) e70798.
[2] C.G. Oliva, N. Jagerovic, P. Goya, I. Alkorta, J. Elguero, R. Cuberes, A. Dordal, N-Substituted-1,2,3-triazoles: synthesis, characterization and evaluation as cannabinoid ligands, Arkivoc (2010) 127–147 ii.
[3] B. Schulze, U.S. Schubert, Beyond click chemistry – supramolecular interactions of 1,2,3-triazoles, Chem. Soc. Rev. 43 (2014) 2522–2571.
[4] S.N. Darandale, N.A. Mulla, D.N. Pansare, J.N. Sangshetti, D.B. Shinde, A novel amalgamation of 1,2,3-triazoles, piperidines and thienopyridine rings and

evaluation of their antifungal activity, Eur. J. Med. Chem. 65 (2013) 527–532.
[5] N. Sangaraiah, S. Murugan, S. Poovan, R. Raja, P. Alagusundaram, V. Ramakrishnan, S. Vellasamy, Facile water promoted synthesis of 1,2,3-triazolyl dihydropyrimidine-2-thione hybrids – highly potent antibacterial agents, Eur. J. Med. Chem. 58 (2012) 464–469.
[6] X.L. Wang, K. Wan, C.H. Zhou, Synthesis of novel sulfanilamide-derived 1,2,3-triazoles and their evaluation for antibacterial and antifungal activities, Eur. J. Med. Chem. 45 (2010) 4631–4639.
[7] S. Shafi, M.M. Alam, N. Mulakayala, C. Mulakayala, G. Vanaja, A.M. Kalle, R. Pallu, M.S. Alam, Synthesis of novel 2-mercapto benzothiazole and 1,2,3-triazole based bis-heterocycles: their anti-inflammatory and anti-nociceptive activities, Eur. J. Med. Chem. 49 (2012) 324–333.
[8] S.P.O. Assis, M.T. Silva, R.N. Oliveira, V.L.M. Lima, Synthesis and anti-inflammatory activity of new alkyl-substituted phthalimide 1H-1,2,3-triazole derivatives, Sci. World J. (2012) 1–7.
[9] D.J. Leaver, R.M. Dawson, J.M. White, A. Polyzos, A.B. Hughes, Synthesis of 1,2,3-triazole linked galactopyranosides and evaluation of cholera toxin inhibition, Org. Biomol. Chem. 9 (2011) 8465–8474.
[10] M.S. Costa, Ń.B. Boechat, E.A. Rangel, F. de C. da Silva, A.M.T. deSouza, C.R. Rodrigues, H.C. Castro, I.N. Junior, M.C.S. Lourenc, S.M.S.V. Wardell, V.F. Ferreira, Synthesis, tuberculosis inhibitory activity, and SAR study of N-substituted-phenyl-1,2,3-triazole derivatives, Bioorg. Med. Chem. 14 (2006) 8644–8653.
[11] A. Özdemir, G. Turan-Zitouni, Z.A. Kaplancıklı, P. Chevallet, Synthesis of some 4-arylidenamino-4H-1,2,4-triazole-3-thiols and their antituberculosis activity, J. Enzym. Inhib. Med. Chem. 22 (2007) 511–516.
[12] A. Kamal, N. Shankaraiah, V. Devaiah, K.L. Reddy, A. Juvekar, S. Sen, N. Kurianb, S. Zingde, Synthesis of 1,2,3-triazole-linked pyrrolobenzodiazepine conjugates employing click chemistry: DNA-binding affinity and anticancer activity, Bioorg. Med. Chem. Lett. 18 (2008) 1468–1473.
[13] A. Kamal, S. Prabhakar, M.J. Ramaiah, P.V. Reddy, Ch R. Reddt, A. Mallareddy, N. Shankaraiah, T.L.N. Reddy, S.N.C.V.L. Pushpavalli, M.P. Bhadra, Synthesis and anticancer activity of chalcone-pyrrolobenzodiazepine conjugates linked via 1,2,3-triazole ring side-armed with alkane spacers, Eur. J. Med. Chem. 46 (2011) 3820–3831.
[14] L.B. Peterson, B.S.J. Blagg, Click chemistry to probe Hsp90: synthesis and evaluation of a series of triazole-containing novobiocin analogues, Bioorg. Med. Chem. Lett. 20 (2010) 3957–3960.
[15] F.D. da Silva, M.C.B.V. de Souza, I.I.P. Frugulhetti, H.C. Castro, S.L.D. Souza, T.M.L. de Souza, D.Q. Rodrigues, A.M.T. Souza, P.A. Abreu, F. Passamani, C.R. Rodrigues, V.F. Ferreira, Synthesis, HIV-RT inhibitory activity and SAR of 1-benzyl-1H-1,2,3-triazole derivatives of carbohydrates, Eur. J. Med.Chem. 44 (2009) 373–383.
[16] M. Whiting, J.C. Tripp, Y.C. Lin, W. Lindstrom, A.J. Olson, J.H. Elder, K.B. Sharpless, Valery V. Fokin, Rapid discovery and Structure–Activity profiling of novel inhibitors of human immunodeficiency virus type 1 protease enabled by the copper(I)-catalyzed synthesis of 1,2,3-Triazoles and their further functionalization, J. Med. Chem. 49 (2006) 7697–7710.
[17] B. Stefane, F. Perdih, A. Visnjevac, F. Pozgan, Novel triazole-based ligands and their zinc(II) and nickel(II) complexes with a nitrogen donor environment as potential structural models for mononuclear active sites, New J. Chem. 39 (2015) 566–575.
[18] G. Aromi, L.A. Barrios, O. Roubeau, P. Gamez, Triazoles and tetrazoles: prime ligands to generate remarkable coordination materials, Coord. Chem. Rev. 255 (2011) 485–546.
[19] C. Richardson, C.M. Fitchett, F.R. Keene, P.J. Steel, 4,5-Di(2-pyridyl)-1,2,3-triazolate: the elusive member of a family of bridging ligandsthat facilitate strong metal–metal interactions, Dalton Trans. (2008) 2534–2546.
[20] A. Maisonial, P. Serafin, M. Traíkia, E. Debiton, V. Thery, D.J. Aitken, P. Lemoine, B. Viossat, A. Gautier, Click chelators for platinum-based anticancer drugs, Eur. J. Inorg. Chem. (2008) 298–305.
[21] K.J. Kilpin, E.L. Gavey, C.J. McAdam, C.B. Anderson, S.J. Lind, C.C. Keep, K.C. Gordon, J.D. Crowley, Palladium(II) complexes of readily functionalized bidentate 2-Pyridyl-1,2,3-triazole "click" ligands: a synthetic, structural, spectroscopic, and computational study, Inorg. Chem. 50 (2011) 6334–6346.
[22] E. Amadio, M. Bertoldini, A. Scrivanti, G. Chessa, V. Beghetto, U. Matteoli, R. Bertani, A. Dolmella, Synthesis, crystal structure, solution behavior and catalytic activity of a palladium(II)-allyl complex containing a 2-pyridyl-1,2,3-triazole bidentate ligand, Inorg. Chim. Acta 370 (2011) 388–393.
[23] C.W. Tornoe, C. Christensen, M. Meldal, Peptidotriazoles on solid phase: [1,2,3]-Triazoles by regiospecific copper(I)-catalyzed 1,3-Dipolar cycloadditions of terminal alkynes to azides, J. Org. Chem. 67 (2002) 3057–3064.
[24] V.V. Rostovsev, L.G. Green, V.V. Fokin, K.B. Sharpless, A stepwise huisgen cycloaddition process: copper(I)-catalyzed regioselective ligation of azides and terminal alkynes, Angew. Chem. Int. Ed. Engl. 41 (2002) 2596–2599.
[25] R. Huisgen, 1,3-Dipolar cycloadditions. Past and future, Angew. Chem. Int. Ed. Engl. 2 (1963) 565–598.
[26] R. Huisgen, Kinetics and mechanism of 1,3-Dipolar cycloadditions, Angew. Chem. Int. Ed. Engl. 2 (1963) 633–645.
[27] N. Belskaya, J. Subbotina, S. Lesogorova, Synthesis of 2H-1,2,3-Triazoles, Top. Heterocycl. Chem. 40 (2015) 51–116.
[28] H. Bauer, A. J. Boulton, A. J. Fedeli, A. R. Katritzky, A. Majid-Hamid, F. Mazza, A.J. Vaciago, N-oxides and related compounds. Part XL. Chemical and X-ray crystallographic investigation of the oxidation products of α-diketone bisacylhydrazones, Chem. Soc. Perkin Trans. II. 662–667.
[29] M. Begtrup, H.P. Nytoft, Reactions of glyoxals with hydrazones: a new route to 4-hydroxypyrazoles, J. Chem. Soc. Perkin Trans. I (1985) 81–90.
[30] M. Begtrup, H.P. Nytoft, 2-Alkyl-1,2,3-Triazole-1-Oxides: preparation and use in the synthesis of 2-Alkyltriazoles, Acta Chem. Scand. B 40 (1986) 262–269.
[31] V.B. Armani, C.D. Erba, M. Novi, G. Petrillo, C. Tavani, Synthetic exploitation of the ring-opening of 3,4-Dinitrothiophene. Part 7. Access to disubstituted 1,2,5-Oxadiazole-2-oxides and 2-Phenyl- 2H-1,2,3-triazole-1-oxides, Tetrahedron 53 (1997) 1751–1758.
[32] M. Begtrup, J. Holm, Electrophilic and nucleophilic substitution in the triazole N-oxides and N-methoxytriazolium salts: preparation of substituted 1,2,3-triazoles, J. Chem. Soc. Perkin Trans. I (1981) 503–511.
[33] H.I. Ucan, R. Mirzaoglu, Synthesis and complex-formation of 6 new unsymmetrical vic-dioximes, Synth. Rect. Inorg. Met. -Org. Chem. 20 (1990) 437–451.
[34] J.J. Norman, R.M. Heggie, J.B. Larose, Oximes: I. The synthesis of some substitited 2-Oximinoacetophenones, Can. J. Chem. 40 (1962) 1547–1553.
[35] N. Koçak, M. Sahin, I. Ucan, The synthesis of two new isonitrosoacetophenone derivatives and investigation of their Ni(II), Co(II), Cu(II), and Zr(IV) complexes, Russ, J. Inorg. Chem. 57 (2012) 1227–1231.
[36] APEX2, SAINT and SADABS, Bruker AXS Inc., Madison, Wisconsin, USA, 2005.
[37] R.H. Blessing, An empirical correction for absorption anisotropy, ActaCryst A51 (1995) 33–38.
[38] G.M. Sheldrick, A short history of SHELX, ActaCryst A64 (2008) 112–122.
[39] L. Farrugia, ORTEP-3 for windows - a version of ORTEP-III with a graphical user interface (GUI), J. Appl. Cryst. 30 (1997), 565–565.
[40] A.L. Spek, Single-crystal Structure Validation with the Program PLATON, a Multipurpose Crystallographic Tool, Utrecht University, Utrecht, The Netherlands, 1998.
[41] L.J. Farrugia, WinGX suite for small-molecule single-crystal crystallography, Appl. Cryst. 32 (1999) 837–838.
[42] J. Marmur, A procedure for the isolation of deoxyribonucleic acid from micro-organisms, J. Mol. Biol. 3 (1961) 208–218.
[43] C.V. Kumar, E.H. Asuncion, DNA binding studies and site selective fluorescence sensitization of an anthryl probe, J. Am. Chem. Soc. 115 (1993) 8547–8553.
[44] M.J. Li, T.Y. Lan, Z.S. Lin, C. Yi, G.N. Chen, Synthesis, characterization, and DNA binding of a novel ligand and its Cu(II) complex, J. Biol. Inorg. Chem. 18 (2013) 993–1003.
[45] K. Dhara, J. Ratha, M. Manassero, X. Wang, S. Gao, P. Banerjee, Synthesis, crystal structure, magnetic property and oxidative DNA cleavage activity of an octanuclear copper(II) complex showing water–perchlorate helical network, J. Inorg. Biochem. 101 (2007) 95–103.
[46] D. Schweinfurth, J. Krzystek, I. Schapiro, S. Demeshko, J. Klein, J. Telser, A. Ozarowski, C.-Y. Su, F. Meyer, M. Atanasov, F. Neese, B. Sarkar, Electronic structures of octahedral Ni(II) complexes with "click" derived triazole ligands: a combined structural, magnetometric, spectroscopic, and theoretical study, Inorg. Chem. 52 (2013) 6880–6892.
[47] R.N. Patel, Y. Singh, Y.P. Singh, R.J. Butcher, Synthesis, crystal structure and DFT calculations of octahedral nickel(II) complexes derived from N′-[(E)-phenyl(pyridin-2- yl)methylidene]benzohydrazide, J. Coord. Chem. 69 (2016) 2377–2390.
[48] M.S. Jana, A.K. Pramanik, T.K. Mondal, Octahedral Ni(II) and Cu(II) complexes with a new hexadentate (NSN)2 donor ligand: synthesis, characterization, X-ray structure and DFT calculations, Polyhedron 76 (2014) 29–35.
[49] Z.-Q. Dong, F.-M. Liu, Y.-M. Zeng, Synthesis and Crystal Structure of new heterocyclic compounds containing 1,2,3-Triazole moiety, J. Chem. Crystallogr. 41 (2011) 1158–1164.
[50] D. Gonzaga, F.C. da Silva, V.F. Ferreira, J.L. Wardell, S.M.S.V. Wardell, Crystal structures of 2-Phenyl-2H-1,2,3-Triazol-4-Carbaldehyde, an active a-glycosidase inhibition agent, and (1-Phenyl-1H-1,2,3- triazol-4-yl)methyl benzoate and (2-(4-Fluorophenyl)-2H-1,2,3- triazole-4-yl)methanol, two moderately active compounds, J. Chem. Crystallogr. 46 (2016) 67–76.
[51] N.R. Madadi, N.R. Penthala, S. Bommagani, S. Parkin, P.A. Crooks, Crystal structure of 4,5-bis(3,4,5-trimethoxyphenyl)-2H-1,2,3-triazole methanol monosolvate, Acta Cryst. E70 (2014) o1128–o1129.
[52] R. Goddard, O. Heinemann, C. Krüger, Pyrrole and a Co-crystal of 1H- and 2H-1,2,3-Triazole, Acta Cryst. C53 (1997) 1846–1850.
[53] R.K. Gupta, R. Pandey, G. Sharma, R. Prasad, B. Koch, S. Srikrishna, P.Z. Li, Q. Xu, D.S. Pandey, Dna binding and Anti-Cancer activity of redox-active heteroleptic piano-stool Ru(II), Rh(III), and Ir(III) complexes containing 4-(2-Methoxypyridyl)phenyldipyrromethene, Inorg. Chem. 52 (2013) 13984–13996.
[54] Q.L. Zhang, J.G. Liu, H. Chao, G.Q. Xue, L.N. Ji, DNA-binding and photocleavage studies of cobalt(III) polypyridyl complexes: [Co(phen)2IP]3+ and [Co(phen)2PIP]3, J. Inorg. Biochem. 83 (2001) 49–55.
[55] F. Mancin, P. Scrimin, P. Tecilla, U. Tonellato, Artificial metallonucleases, Chem. Commun. (2005) 2540–2548.
[56] L. Tjioe, A. Meininger, T. Joshi, L. Spiccia, B. Graham, Efficient plasmid DNA cleavage by copper(ii) complexes of 1,4,7-Triazacyclononane ligands featuring Xylyl-linked guanidinium groups, Inorg. Chem. 50 (2011) 4327–4339.
[57] E.C. Long, J.K. Barton, On demonstrating DNA intercalation, Acc. Chem. Res. 23 (1990) 271–273.
[58] R. Eshkourfu, B. Čobeljić, M. Vujčić, I. Turel, A. Pevec, K. Sepčić, M. Zec, S. Radulović, T. Srdić-Radić, D. Mitić, K. Andjelković, D. Sladić, Synthesis, characterization, cytotoxic activity and DNA binding properties of the novel dinuclear cobalt(III) complex with the condensation product of 2-

acetylpyridine and malonic acid dihydrazide, J. Inorg. Biochem. 105 (2011) 1196–1203.
[59] Y.N. Xiao, C.X. Zhan, Studies on the interaction of DNA and water-soluble polymeric Schiff base–nickel complexes, J. Appl. Polym. Sci. 84 (2002) 887–893.
[60] S. Satyanarayana, J.C. Dabrowiak, J.B. Chaires, Tris(phenanthroline)ruthenium(II) enantiomer interactions with DNA: mode and specificity of binding, Biochemistry 32 (1993) 2573–2584.
[61] K.E. Reinert, Aspects of specific DNA-protein interaction; localbending of DNA molecules by in-register binding of the oligopeptideantibioticdistamycin, Biophys. Chem. 13 (1981) 1–14.
[62] B. Liao, H.Y. Zhou, X.M. Xiao, Spectroscopic and viscosity study of doxorubicin interaction with DNA, J. Molec. Struct. 749 (2005) 108–113.
[63] G. Cohen, H. Einsenberg, Viscosity and sedimentation study of sonicated DNA–proflavine complexes, Biopolymers 8 (1969) 45–55.